BELLE-CONF-0007
Parallel Session: PA-07
Plenary Session: PL-01b
Revised on 2000/07/24

Evidence for the charmless decay $B^+ \to \phi K^+$ at Belle

The Belle Collaboration

Abstract

We report on a search for two-body charmless decays $B^+/B^0 \to \phi(1020)K$ using a sample of $\sim 5.5 \times 10^6$ of $B\bar{B}$ pairs recorded at the $\Upsilon(4S)$ resonance with the Belle detector at the KEKB e^+e^- storage ring. We report evidence for $B^+ \to \phi(1020)K^+$ and determine a branching fraction. The results are preliminary.

A. Abashian[44], K. Abe[8], K. Abe[36], I. Adachi[8], Byoung Sup Ahn[14], H. Aihara[37], M. Akatsu[19], G. Alimonti[7], K. Aoki[8], K. Asai[20], M. Asai[9], Y. Asano[42], T. Aso[41], V. Aulchenko[2], T. Aushev[12], A. M. Bakich[33], E. Banas[15], S. Behari[8], P. K. Behera[43], D. Beiline[2], A. Bondar[2], A. Bozek[15], T. E. Browder[7], B. C. K. Casey[7], P. Chang[23], Y. Chao[23], B. G. Cheon[32], S.-K. Choi[6], Y. Choi[32], Y. Doi[8], J. Dragic[17], A. Drutskoy[12], S. Eidelman[2], Y. Enari[19], R. Enomoto[8,10], C. W. Everton[17], F. Fang[7], H. Fujii[8], K. Fujimoto[19], Y. Fujita[8], C. Fukunaga[39], M. Fukushima[10], A. Garmash[2,8], A. Gordon[17], K. Gotow[44], H. Guler[7], R. Guo[21], J. Haba[8], T. Haji[4], H. Hamasaki[8], K. Hanagaki[29], F. Handa[36], K. Hara[27], T. Hara[27], T. Haruyama[8], N. C. Hastings[17], K. Hayashi[8], H. Hayashii[20], M. Hazumi[27], E. M. Heenan[17], Y. Higashi[8], Y. Higasino[19], I. Higuchi[36], T. Higuchi[37], T. Hirai[38], H. Hirano[40], M. Hirose[19], T. Hojo[27], Y. Hoshi[35], K. Hoshina[40], W.-S. Hou[23], S.-C. Hsu[23], H.-C. Huang[23], Y.-C. Huang[21], S. Ichizawa[38], Y. Igarashi[8], T. Iijima[8], H. Ikeda[8], K. Ikeda[20], K. Inami[19], Y. Inoue[26], A. Ishikawa[19], R. Itoh[8], G. Iwai[25], M. Iwai[8], H. Iwasaki[8], Y. Iwasaki[8], D. J. Jackson[27], P. Jalocha[15], H. K. Jang[31], M. Jones[7], R. Kagan[12], H. Kakuno[38], J. Kaneko[38], J. H. Kang[45], J. S. Kang[14], P. Kapusta[15], K. Kasami[8], N. Katayama[8], H. Kawai[3], M. Kawai[8], N. Kawamura[1], T. Kawasaki[25], H. Kichimi[8], D. W. Kim[32], Heejong Kim[45], H. J. Kim[45], Hyunwoo Kim[14], S. K. Kim[31], K. Kinoshita[5], S. Kobayashi[30], S. Koike[8], Y. Kondo[8], H. Konishi[40], K. Korotushenko[29], P. Krokovny[2], R. Kulasiri[5], S. Kumar[28], T. Kuniya[30], E. Kurihara[3], A. Kuzmin[2], Y.-J. Kwon[45], M. H. Lee[8], S. H. Lee[31], C. Leonidopoulos[29], H.-B. Li[11], R.-S. Lu[23], Y. Makida[8], A. Manabe[8], D. Marlow[29], T. Matsubara[37], T. Matsuda[8], S. Matsui[19], S. Matsumoto[4], T. Matsumoto[19], K. Misono[19], K. Miyabayashi[20], H. Miyake[27], H. Miyata[25], L. C. Moffitt[17], G. R. Moloney[17], G. F. Moorhead[17], N. Morgan[44], S. Mori[42], T. Mori[4], A. Murakami[30], T. Nagamine[36], Y. Nagasaka[18], Y. Nagashima[27], T. Nakadaira[37], T. Nakamura[38], E. Nakano[26], M. Nakao[8], H. Nakazawa[4], J. W. Nam[32], S. Narita[36], Z. Natkaniec[15], K. Neichi[35], S. Nishida[16], O. Nitoh[40], S. Noguchi[20], T. Nozaki[8], S. Ogawa[34], R. Ohkubo[8], T. Ohshima[19], Y. Ohshima[38], T. Okabe[19], T. Okazaki[20], S. Okuno[13], S. L. Olsen[7], W. Ostrowicz[15], H. Ozaki[8], P. Pakhlov[12], H. Palka[15], C. S. Park[31], C. W. Park[14], H. Park[14], L. S. Peak[33], M. Peters[7], L. E. Piilonen[44], E. Prebys[29], J. Raaf[5], J. L. Rodriguez[7], N. Root[2], M. Rozanska[15], K. Rybicki[15], J. Ryuko[27], H. Sagawa[8], Y. Sakai[8], H. Sakamoto[16], H. Sakaue[26], M. Satapathy[43], N. Sato[8], A. Satpathy[8,5], S. Schrenk[44], S. Semenov[12], Y. Settai[4], M. E. Sevior[17], H. Shibuya[34], B. Shwartz[2], A. Sidorov[2], V. Sidorov[2], S. Stanič[42], A. Sugi[19], A. Sugiyama[19], K. Sumisawa[27], T. Sumiyoshi[8], J. Suzuki[8], J.-I. Suzuki[8], K. Suzuki[3], S. Suzuki[19], S. Y. Suzuki[8], S. K. Swain[7], H. Tajima[37], T. Takahashi[26], F. Takasaki[8], M. Takita[27], K. Tamai[8], N. Tamura[25], J. Tanaka[37], M. Tanaka[8], Y. Tanaka[18], G. N. Taylor[17], Y. Teramoto[26], M. Tomoto[19], T. Tomura[37], S. N. Tovey[17], K. Trabelsi[7], T. Tsuboyama[8], Y. Tsujita[42], T. Tsukamoto[8], T. Tsukamoto[30], S. Uehara[8], K. Ueno[23], N. Ujiie[8], Y. Unno[3], S. Uno[8], Y. Ushiroda[16], Y. Usov[2], S. E. Vahsen[29], G. Varner[7], K. E. Varvell[33], C. C. Wang[23], C. H. Wang[22], M.-Z. Wang[23], T.-J. Wang[11], Y. Watanabe[38], E. Won[31], B. D. Yabsley[8], Y. Yamada[8], M. Yamaga[36], A. Yamaguchi[36], H. Yamaguchi[8], H. Yamamoto[7], H. Yamaoka[8], Y. Yamaoka[8], Y. Yamashita[24], M. Yamauchi[8], S. Yanaka[38], M. Yokoyama[37], K. Yoshida[19], Y. Yusa[36], H. Yuta[1], C.-C. Zhang[11], H. W. Zhao[8], Y. Zheng[7], V. Zhilich[2], and D. Žontar[42]

[1]Aomori University, Aomori

[2]Budker Institute of Nuclear Physics, Novosibirsk
[3]Chiba University, Chiba
[4]Chuo University, Tokyo
[5]University of Cincinnati, Cincinnati, OH
[6]Gyeongsang National University, Chinju
[7]University of Hawaii, Honolulu HI
[8]High Energy Accelerator Research Organization (KEK), Tsukuba
[9]Hiroshima Institute of Technology, Hiroshima
[10]Institute for Cosmic Ray Research, University of Tokyo, Tokyo
[11]Institute of High Energy Physics, Chinese Academy of Sciences, Beijing
[12]Institute for Theoretical and Experimental Physics, Moscow
[13]Kanagawa University, Yokohama
[14]Korea University, Seoul
[15]H. Niewodniczanski Institute of Nuclear Physics, Krakow
[16]Kyoto University, Kyoto
[17]University of Melbourne, Victoria
[18]Nagasaki Institute of Applied Science, Nagasaki
[19]Nagoya University, Nagoya
[20]Nara Women's University, Nara
[21]National Kaohsiung Normal University, Kaohsiung
[22]National Lien-Ho Institute of Technology, Miao Li
[23]National Taiwan University, Taipei
[24]Nihon Dental College, Niigata
[25]Niigata University, Niigata
[26]Osaka City University, Osaka
[27]Osaka University, Osaka
[28]Panjab University, Chandigarh
[29]Princeton University, Princeton NJ
[30]Saga University, Saga
[31]Seoul National University, Seoul
[32]Sungkyunkwan University, Suwon
[33]University of Sydney, Sydney NSW
[34]Toho University, Funabashi
[35]Tohoku Gakuin University, Tagajo
[36]Tohoku University, Sendai
[37]University of Tokyo, Tokyo
[38]Tokyo Institute of Technology, Tokyo
[39]Tokyo Metropolitan University, Tokyo
[40]Tokyo University of Agriculture and Technology, Tokyo
[41]Toyama National College of Maritime Technology, Toyama
[42]University of Tsukuba, Tsukuba
[43]Utkal University, Bhubaneswer
[44]Virginia Polytechnic Institute and State University, Blacksburg VA
[45]Yonsei University, Seoul

I. INTRODUCTION

Decays involving $b \to ss\bar{s}$ transitions such as $B \to \phi(1020)K$ cannot occur via a tree process and are expected to be dominated by the penguin diagram, thus their measurement will give information on the strength of the penguin transition. Upper limits for $B \to \phi K$ decays channels have been set by the CLEO experiment in data samples with integrated luminosities of 2.42 [1], 3.11 [2] and 5.5 fb^{-1} [3] . The current best 90% C.L. upper limits for the branching fractions of $B^{\pm} \to \phi K^{\pm}$ and $B^0 \to \phi K^0$ decays are 0.59×10^{-5} and 2.8×10^{-5} respectively [3].

The results reported here are based on a data sample recorded with the Belle detector [4] at the KEKB e^+e^- accelerator [5] operating at the $\Upsilon(4S)$ resonance. The data sample contains about $5.5 \times 10^6 B\bar{B}$ pairs.

The KEKB accelerator is a double ring asymmetric storage ring with 8 GeV electrons and 3.5 GeV positrons. Asymmetric collisions result in a small boost of $B\bar{B}$ pairs along the beam line.

The Belle detector is a general purpose magnetic spectrometer equipped with a 1.5 T superconducting solenoid magnet. Charged tracks are reconstructed in a 50 layer Central Drift Chamber (CDC) [6] and in three concentric layers of double sided silicon strip detectors of the Silicon Vertex Detector (SVD) [7]. The charged particle acceptance of the spectrometer covers the laboratory polar angles $17^\circ < \theta < 150^\circ$ which corresponds to $\sim 90\%$ of the full CMS solid angle. The momentum resolution is determined from cosmic rays and $e^+e^- \to \mu^+\mu^-$ events to be $\sigma_{p_t}/p_t = (0.36 \oplus 0.28 p_t)\%$, where p_t is the transverse momentum in GeV. Photons and electrons are identified using the CsI(Tl) Electromagnetic Calorimeter (ECL) [8] located inside the magnet coil. Muons and K_L^0's are detected using resistive plate chambers embedded in the iron magnetic flux return (KLM) [11]. Charged particles are identified using specific ionization losses in the CDC and identification information from the Aerogel Cherenkov Counters (ACC) [9] and Time of Flight Counters (TOF) [10]. By these three methods, K/π separation is achieved over the momentum range from about 0.2 to 3.5 GeV. The high momentum kaon identification efficiency is measured to be $\sim 80\%$ [9].

II. EVENT SELECTION

We study the following two final state topologies:

$$\begin{array}{ll} B^+ \to \phi(1020)K^+ & \text{where } \phi \to K^+K^-, \\ B^0 \to \phi(1020)K_s^0 & \text{where } \phi \to K^+K^-,\ K_S^0 \to \pi^+\pi^- \end{array}$$

(the inclusion of the charge conjugate states is always implied in this report). In the search for the above channels we take full advantage of asymmetric e^+e^- collisions resulting in boosted $B\bar{B}$ pairs and the good vertexing and particle identification capabilities of the Belle detector.

We search for $\phi(1020) \to K^+K^-$ decays by selecting pairs of oppositely charged tracks that are well measured in the SVD and have a minimum level of positive kaon identification (which selects kaons with $> 90\%$ efficiency). The candidate kaon pairs are required to pass a vertex fit with a beam spot constraint ($\sigma_x \approx 100\,\mu$m , $\sigma_y \approx 5\,\mu$m and $\sigma_z \approx 3$ mm) enlarged by a halo corresponding to the width expected for the B meson lifetime (≈ 20 μm in the

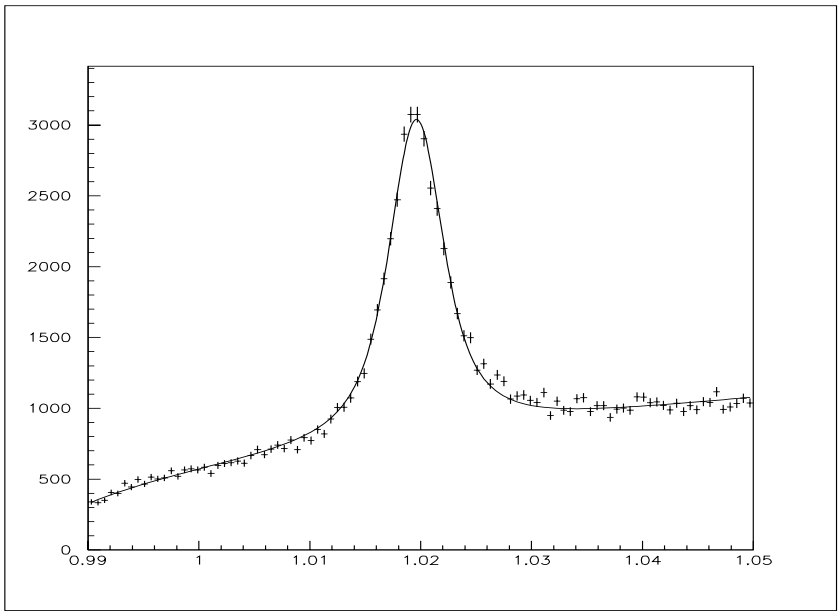

FIG. 1. The K^+K^- ($p^*_{KK} > 2\,\mathrm{GeV}$) invariant mass distribution in the $\phi(1020)$ region. The superimposed curve : the result of the fit with a Breit-Wigner formula convoluted with a Gaussian describing mass resolution and a polynomial and threshold terms describing background. Γ_ϕ was fixed at the PDG value. Fitted mass $m_\phi = 1019.6 \pm 0.4\,\mathrm{MeV}$, and resolution $\sigma = 1.2 \pm 0.1\,\mathrm{MeV}$

transverse plane). A run dependent Interaction Point (IP) position and Beam Spot (BS) size are used in the fit. No cuts on the $\phi(1020)$ vertex quality are made: only the convergence of the fit is required. This procedure slightly enhances the position and mass resolutions for pairs of tracks with small opening angles, and rejects secondary vertices not compatible with the primary vertex of the event. Events with a candidate $\phi(1020)$ are accepted if the ϕ momentum in the CMS exceeds 2.0 GeV. The momentum cut value is based on the approximate monochromaticity of the B decay products in a two-body decay and takes into account the B momentum spread in the $\Upsilon(4S)$ CMS. This cut is 100% efficient for all final states studied. It effectively suppresses ϕ mesons from B cascade decays, and reduces the continuum background by a factor of 3. The $\phi(1020)$ invariant mass distribution for selected events is shown in Fig. 1.

In events where the K^+K^- invariant mass is in the $\phi(1020)$ mass window $|m_{KK} - m_\phi| < 0.010\,\mathrm{GeV}$, a search is made for the second B decay product, $K^\pm$ or K^0_S. For charged kaons $K^\pm$, the required level of particle identification is optimized using the measured kaon efficiency and pion misidentification curves: at the chosen cut value the kaon identification efficiency exceeded 80%. For $K^0_S \to \pi^+\pi^-$ decays we use oppositely charged track pairs where the displacement of the $\pi^+\pi^-$ vertex from the interaction region in the transverse $(r-\phi)$ plane is more than 1 mm and the ϕ coordinate of the $\pi^+\pi^-$ vertex point and the ϕ direction of the $\pi^+\pi^-$ candidate's momentum vector agree within 0.2 radians and $|m_{\pi\pi} - m_{K^0}| < 15\,\mathrm{MeV}$.

For the accepted candidates, a vertex fit of the $\phi(1020)$ decay products and the K candidate is performed using the BS constraint described above, to test compatibility of the vertex with the interaction region. No cut is made on the vertex quality or the distance of

the vertex from the IP.

To suppress $q\bar{q}$ continuum background, cuts are applied on the angle between the B candidate momentum vector and the thrust vector of the remaining tracks of the event ($|\cos(\theta_{thr-B})| < 0.8$) and on the B candidate production angle in the CMS ($|\cos(\theta^*_B)| < 0.8$). We also require $|\cos(\theta_H)| > 0.5$ where the helicity angle θ_H is the angle between the direction of the K^+ and the momentum vector of $\phi(1020)$, in the ϕ rest frame*.

III. RESULTS

For each $B \to \phi K$ candidate event the beam constrained mass is calculated, $M_b = \sqrt{E^{*2}_{beam} - p^{*2}_B}$, where p^*_B is the B candidate momentum and E^*_{beam} is half the CMS energy. The resolution in the beam constrained mass is an order of magnitude better than the invariant mass resolution. The energy difference is defined as $\Delta E = E^*_\phi + E^*_K - E^*_{beam}$, where E^*_ϕ and E^*_K are the measured $\phi(1020)$ and K energies in the CMS; the $\sim 3\,\mathrm{MeV}$ variation in E^*_{beam} between different running periods is taken into account in the calculations. The signal region is defined in the ΔE vs. M_b plane by a box with $\Delta E = \pm 64\,\mathrm{MeV}$ (3 times the expected resolution) and $M_b > 5.270\,\mathrm{GeV}$.

A. $B^\pm \to \phi K^\pm$

The ΔE vs M_b distribution for candidates that pass the cuts is shown in Fig. 2(b). Eleven candidates fall into the 3σ signal box with a modest background of 58 events outside. An accumulation of events in the signal box can be clearly seen. The M_b projection for background events in the upper sideband of ΔE ($100\,\mathrm{MeV} < \Delta\mathrm{E} < 300\,\mathrm{MeV}$) is shown in Fig. 3(a). The $\Delta E < -100\,\mathrm{MeV}$ sideband is not used for background studies because other $B \to \phi(1020)KX$ decays with undetected particles could contribute to this region. The background shape is rather flat and does not show any accumulation in the signal region. The background shape for the sideband events from a sample with looser selection cuts is shown in Fig. 3(b). This distribution is used to fix the shape parameter of the ARGUS function†, which we use to parametrize the background when fitting the M_b distribution in the signal region.

The largest background contribution to the signal region comes from continuum $q\bar{q}$ production where a high momentum $\phi(1020)$ from one jet is randomly combined with a high momentum kaon from another jet, with a momentum balance within the range kinematically allowed for B mesons. The amount of this background is estimated using a continuum data sample of $0.6\,\mathrm{fb}^{-1}$ taken 60 MeV below the $\Upsilon(4S)$ peak and 25×10^6 continuum MC events.

---

*In a Pseudoscalar(P) $\to$ Pseudoscalar - Vector(V) decay the vector meson is polarized, decaying to two pseudoscalars $V \to PP$ according to a $\cos^2(\theta_H)$; the combinatorial bacground is flat in $\cos(\theta_H)$.

†$B(x) = N\sqrt{1-x^2}\exp(P(1-x^2))$; where $x = \frac{M_b}{E^*_{beam}}$, P is the shape variable fitted to background sample and N is the overall normalization factor fitted to the distribution in the signal region.

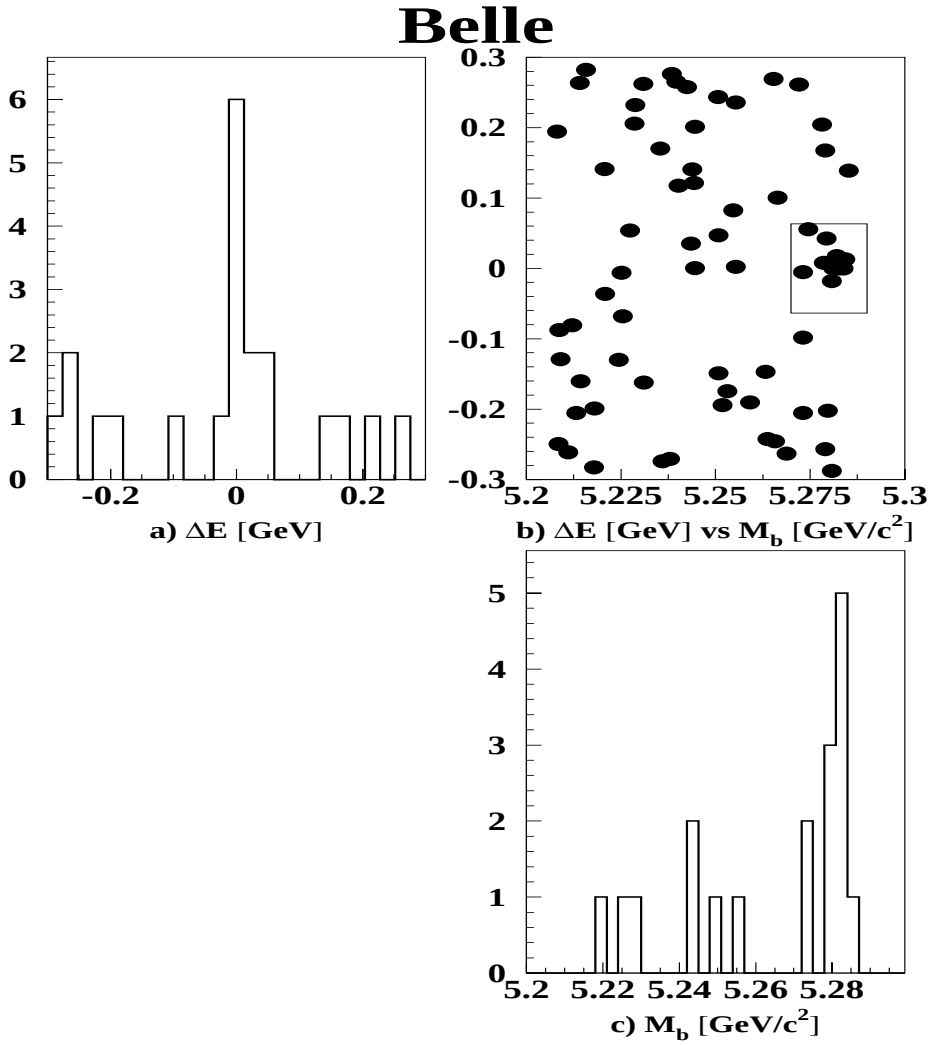

FIG. 2. (a) The ΔE projection, (b) ΔE vs M_b for selected $B^{\pm} \to \phi(1020)K^{\pm}$ candidates, the box represents the $\pm 3\sigma$ signal region; (c) the M_b projection.

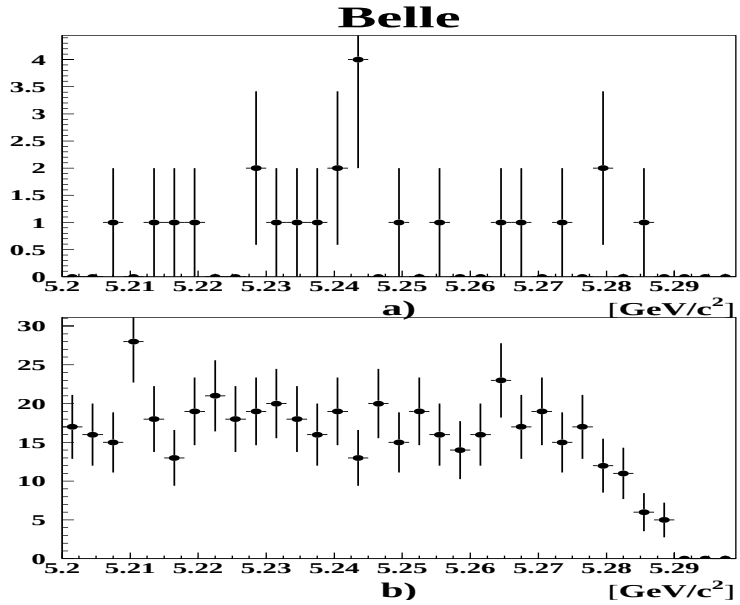

FIG. 3. (a) The M_b distribution for events from the sideband with 100 MeV $<\Delta$E$<$ 300 MeV; (b) the M_b distribution for the background enriched sample (no cuts on $\cos(\theta_H)$ or $\cos(\theta^*_B)$, looser KID requirements for kaons coming from $\phi(1020)$ and $|\cos(\theta_{thr-B})| > 0.8$)

The background prediction from the continuum data agrees within errors with the amount of the observed background. The MC prediction in the full ΔE vs. M_b plane is higher by 30% (a 3σ discrepancy). The background shape for continuum is shown in Fig.4.

Other background sources such $B \to \phi(1020)K^*$ decays with missing or misidentified pions, combinatorial background from generic B or from rare B decays have been studied with large MC data sets and found to be negligible.

The results of a binned likelihood fit to the M_b distribution in the $\Delta E < \pm 3\sigma$ band are summarized in Table I and are shown in Fig.5. The free parameters of the fit are the number of signal and background events, and the B meson mass. The width of the signal is fixed at the expected value of 3.0 MeV. In some variants of the fit this width was allowed to vary: this did not change the results. The stability of the fit results has been checked by changing the background shape parameterization and choosing different sideband regions to estimate its parameters. The resulting variations of the fit results are used for systematic error estimation.

TABLE I. Fit results : n_S is the yield of fitted signal candidates, n_B is the background in a region $\pm 3\sigma$ around the peak position

	n_S	n_B	M_B (MeV)	σ_{M_B}(MeV)
$B^\pm \to \phi K^\pm$	$9.2^{+3.6}_{-2.9}$	1.0 ± 0.4	5281.0 ± 1.0	$3.0(fixed)$

The result of an independent fit of a Gaussian form and a constant background term to the ΔE projection for $M_b > 5.270$ GeV is shown in Fig. 6. In this fit the width of the Gaussian is fixed to the measured ΔE resolution $\sigma_{\Delta E} = 21$ MeV. The fit yields a number

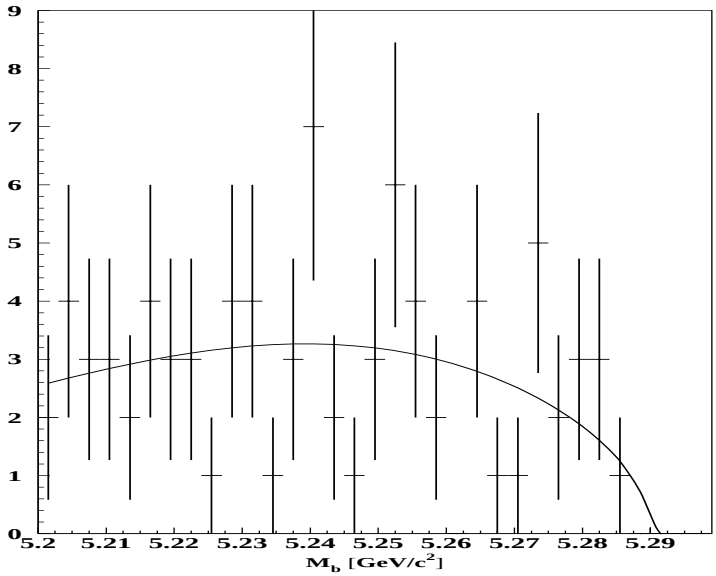

FIG. 4. The M_b distribution from 25×10^6 MC continuum events. Events in the plot passed the same selection cuts as the data. The distribution shown is for $\Delta E < 5\sigma$ for better statistics; the distribution for $\Delta E < 3\sigma$ has the same features.

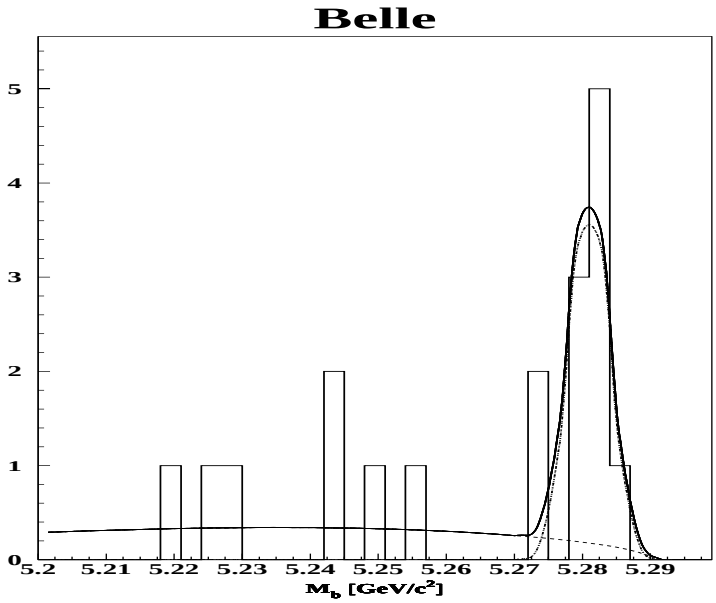

FIG. 5. The fit to the M_b projection for $\Delta E < 3\sigma$ in data

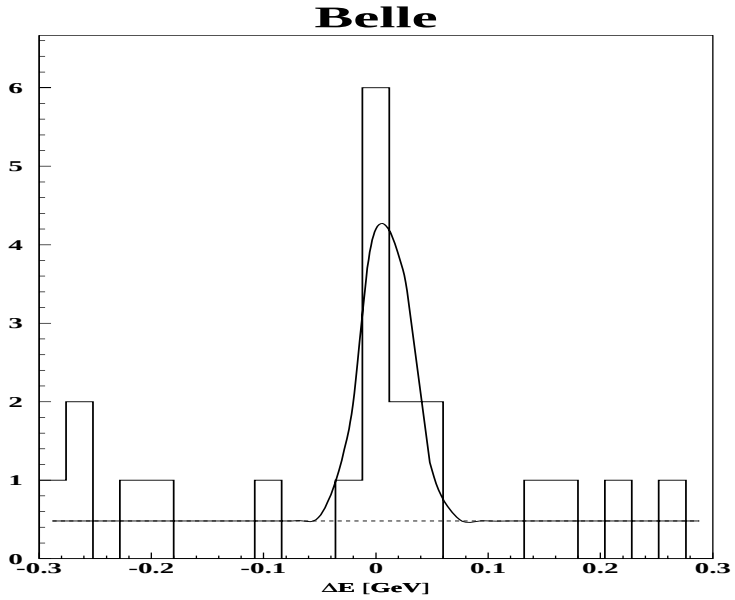

FIG. 6. The fit to the ΔE projection for $M_b > 5.270\,\mathrm{GeV}$.

of signal events, $n_S = 9.0^{+3.7}_{-3.0}$, which is in a good agreement with the result of the M_b fit. The prediction for the number of background events is higher ($n_B = 2.5 \pm 0.75$) but still consistent with the M_b fit results.

Additional studies of systematics were done to check if variations of the number of signal events follow the expected efficiency changes. By tightening or loosening the selection cuts, the M_b distribution has been accordingly depleted or enriched with background. The number of signal events behaved accordingly to the evaluated selection efficiency changes. An example is shown in Fig.7 for the selection that has the efficiency increased by 35%.

The final result for the number of signal events is :

$$n_S = 9.2^{+3.6}_{-2.9} \pm 0.8$$

and for the number of background events is :

$$n_B = 1.0 \pm 0.4 \pm 0.4,$$

where the second error terms represent systematic errors from background parameterization and different σ_{m_B} assumed in the fit.

Considering statistical errors alone, the n_S result is statistically significant, as can be seen from the following approximate calculations:

- From the likelihood profile of the fit as a function of n_S, we find that $-2ln(L)$ increases by 29.0 from the function minimum to $n_S = 0$, corresponding to a $5.4\,\sigma$ effect.
- Treating these fit results as the measurement of a number of events in a single bin over a known background, we can apply the Feldman-Cousins method for estimating a confidence interval [12]. For an observation of 10.2 events ($n_S + n_b$) with an expected background of 1.0, the 90% confidence interval on n_S is $4.6 < n_S < 15.8$.

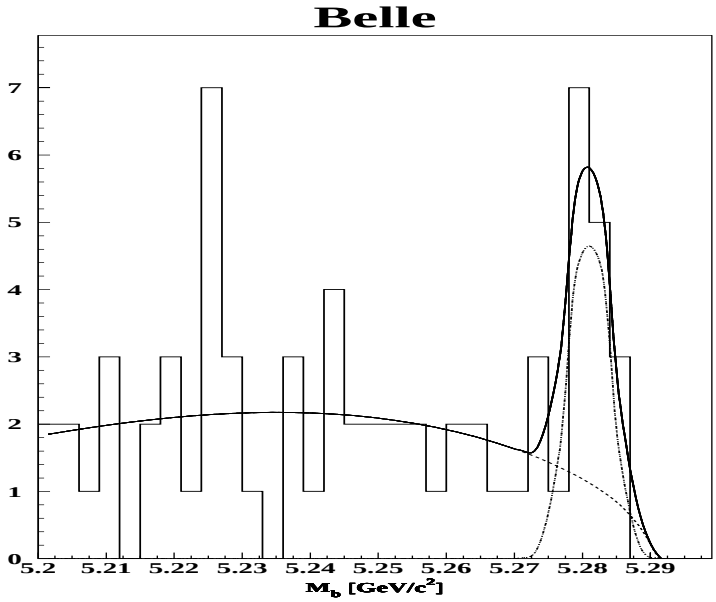

FIG. 7. The fit to the M_b projection for $\Delta E < 3\sigma$ for events selected with looser selection cuts (no cuts on $\cos(\theta_H)$ or $cos(\theta^*_B)$ and $|\cos(\theta_{thr-B})| < 0.9$). The efficiency is 35% higher than the standard cuts.

- The fit to the ΔE distribution gives similar statistical significance.

Studies of systematic effects are still preliminary. The effects of present systematic estimates may be judged by repeating the Feldman-Cousins calculation after lowering the observed signal, and increasing the observed background, by the systematic errors. For an observation of 9.8 events over an expected background of 1.4 events, the 90% confidence interval for n_S is $3.8 < n_S < 15.9$, which does not include zero.

B. $B^0 \to \phi K^0$

Candidates that pass the $B^0 \to \phi K^0_S$ selection criteria are shown in Fig. 8. There are two candidates in the signal box. The number of background events estimated from the ΔE vs. M_B region outside the box is 0.4 ± 0.2 events. No significant signal is observed. The product of the detection efficiency and all relevant branching fractions for this decay channel is four times lower than in the case of $B^+ \to \phi K^+$. Based on the observed number of signal events in the charged channel, the ratio of detector efficiencies for both channels and assuming isospin invariance of the B decay, 2.4 ± 0.7 events are expected in the ϕK^0_S mode; the observed number of candidates is compatible with this prediction.

IV. BRANCHING FRACTION RESULTS

The detection efficiency, as determined from the MC simulation, has been corrected for known differences between the MC and the data. A tracking efficiency correction for the

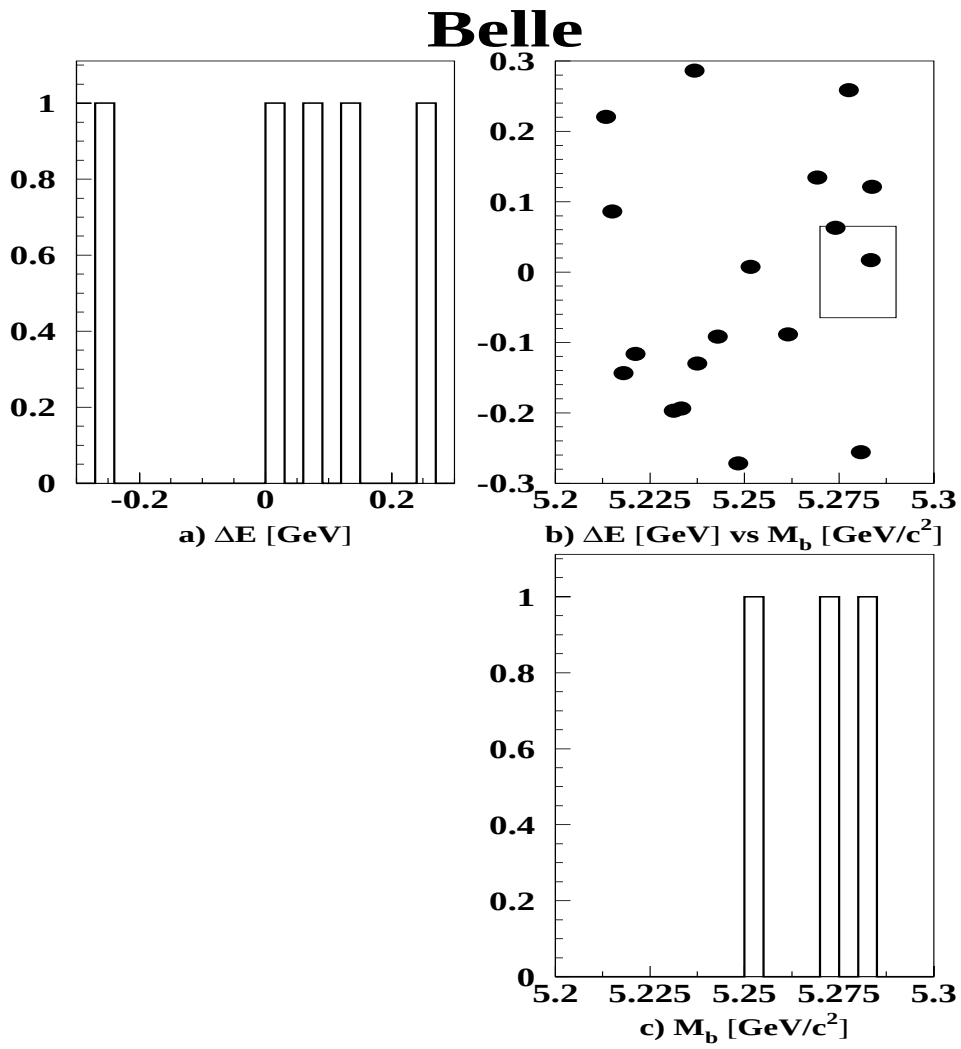

FIG. 8. (a) The ΔE projection, (b) ΔE vs M_b for selected $B^0 \to \phi K^0_S$ candidates, the box represents the $\pm 3\sigma$ signal region; (c) the M_b projection.

MC was obtained from studies of $\eta \to \pi^+\pi^-\pi^0$ and $\eta \to \gamma\gamma$ and is found to be 1.012 ± 0.045 for high momentum charged pions. The kaon identification efficiency measured in the real data for selected $\phi(1020)$ signal events has been used. The discrepancy between the particle identification efficiency for simulated data and real data has been corrected for. The correction factor for kaons from $\phi(1020) \to K^+K^-$ decays is determined to be 0.929 ± 0.013 and that for the kaon from the B decay is calibrated from $D^{*+} \to D^0(K\pi)\pi^+$ decays to be 0.87 ± 0.01. The estimated product of the detection efficiency and $(\mathcal{B}(\phi) \to K^+K^-)$ is equal to $9.7 \pm 0.6\%$.

For the branching fraction calculation equal $\Upsilon(4S)$ decay rates to B^+B^- and $B^0\bar{B}^0$ are assumed. We obtain a preliminary value of

$$\mathcal{B}(B^\pm \to \phi(1020)K^\pm) = (1.72^{+0.67}_{-0.54} \pm 0.18) \times 10^{-5} \ .$$

This result can be also expressed as a 90% confidence interval determined by the procedure described above :

$$0.71 \times 10^{-5} < \mathcal{B}(B^\pm \to \phi(1020)K^\pm) < 3.0 \times 10^{-5},$$

based on statistical errors only (the central value of the detection efficiency has been used).

V. CONCLUSIONS

We report the first evidence for charmless $B^+ \to \phi(1020)K^+$ decays. A signal of $9.2^{+3.6}_{-2.9} \pm 0.8$ events has been observed over a low background. The corresponding branching fraction is only marginally compatible with the CLEO 90% C.L. upper limit [3]. Phenomenological predictions for this branching fraction span a wide range (see [13], [14], [15], [16], [17]), and there are predictions that accomodate our result.

No significant signal is observed for $B^0 \to \phi K^0$, but this channel has 4 times lower effective detection efficiency then $B^+ \to \phi(1020)K^+$.

The results presented here are still preliminary.

VI. ACKNOWLEDGMENTS

We gratefully acknowledge the efforts of the KEKB group in providing us with excellent luminosity and running conditions and the help with our computing and network systems provided by members of the KEK computing research center. We thank the staffs of KEK and collaborating institutions for their contributions to this work, and acknowledge support from the Ministry of Education, Science, Sports and Culture of Japan and the Japan Society for the Promotion of Science; the Australian Research Council and the Australian Department of Industry, Science and Resources; the Department of Science and Technology of India; the BK21 program of the Ministry of Education of Korea and the Basic Science program of the Korea Science and Engineering Foundation; the Polish State Committee for Scientific Research under contract No.2P03B 17017; the Ministry of Science and Technology of Russian Federation; the National Science Council and the Ministry of Education of Taiwan; the Japan-Taiwan Cooperative Program of the Interchange Association; and the U.S. Department of Energy.

REFERENCES

[1] CLEO Collaboration, D.M.Asner et al., CLNS 95/1338, CLEO 95-8 (July 1999)
[2] CLEO Collaboration, T.Bergfeld et al., CLNS 97/1537, CLEO 97-32 (May 2000)
[3] CLEO Collaboration, M.Bishai et al., CLEO CONF 99-13 (August 1999)
[4] Belle Collaboration, Technical Design Report, KEK Report 95-1, 1995.
[5] KEKB accelerator group, KEKB B Factory Design Report, KEK Report 95-7, 1995.
[6] H. Hirano *et al.*, KEK Preprint 2000-2, submitted to Nucl. Inst. Meth.; M. Akatsu *et al.*, DPNU-00-06, submitted to Nucl. Inst. Meth.
[7] G. Alimonti *et al.*, KEK preprint 2000-34.
[8] H. Ikeda *et al.*, Nucl. Inst. Meth. **441**, 401 (2000).
[9] T. Iijima *et al.*, Proceedings of the 7th International Conference on Instrumentation for Colliding Beam Physics, Hamamatsu, Japan, Nov 15-19, 1999.
[10] H. Kichimi *et al.*, submitted to Nucl. Inst. Meth.
[11] A. Abashian *et al.*, Nucl. Instr. Meth. **A449**, 112 (2000).
[12] G.J.Feldman, R.D.Cousins, Phys. Rev. D **57**, 7 (1998).
[13] N.G. Deshpande and J.Trampetic, Phys. Rev. D **41**, 895 (1990).
[14] L.-L. Chau *et al.*, Phys. Rev. D **43**, 2176 (1991).
[15] A. Deandrea, N. Di Bartolomeo, and R. Gatto, Phys. Lett. B **318**, 549 (1993); A.Deandrea *et al.Phys. Lett. B* **320***, 170 (1994).*
[16] W.S.Hou *et al.*, hep-exp/9910014 (1999).
[17] H.Y.Cheng, K-Ch.Yang, hep-ph/9910291 (2000).